

Development and application of a neural network based coating weight control system for a hot-dip galvanizing line

Zai-sheng PAN^{†‡1}, Xuan-hao ZHOU², Peng CHEN²

¹*Institute of Cyber-Systems and Control, Zhejiang University, Hangzhou 310027, China*

²*Zhejiang SUPCON Research Co., Ltd., Hangzhou 310053, China*

[†]E-mail: panzs@zju.edu.cn

Received July 6, 2016; Revision accepted Sept. 19, 2016; Crosschecked July 8, 2018

Abstract: The hot-dip galvanizing line (HDGL) is a typical order-driven discrete-event process in steelmaking. It has some complicated dynamic characteristics such as a large time-varying delay, strong nonlinearity, and unmeasured disturbance, all of which lead to the difficulty of an online coating weight controller design. We propose a novel neural network based control system to solve these problems. The proposed method has been successfully applied to a real production line at VaLin LY Steel Co., Loudi, China. The industrial application results show the effectiveness and efficiency of the proposed method, including significant reductions in the variance of the coating weight and the transition time.

Key words: Neural network; Hot-dip galvanizing line (HDGL); Coating weight control

<https://doi.org/10.1631/FITEE.1601397>

CLC number: TP273; TP183

1 Introduction


Hot-dip coating is a popular production process after cold milling in steelmaking. This process produces high value-added products such as galvanized sheet, which is widely used in automotive and household electrical appliance manufacturing (Jordan et al., 1993; Marder, 2000). In recent years, studies that incorporate control and information technology to realize online coating weight control systems have been an attractive research area. A general schematic diagram of a typical hot-dip galvanizing line (HDGL) is shown in Fig. 1.

As shown in Fig. 1a, the strip receives heat treatment in an annealing furnace, and then passes through a molten zinc bath where hot liquid zinc is attached to the surface of the strip. The deposited coating weight on the strip is controlled by the air

knife installed just above the zinc pot and close to the liquid level. After that, the strip passes through a series of auxiliary processes, such as leveling, passivation, oiling, and finally being wound into a coil. As shown in Fig. 1b, a typical air knife includes two identical parts, a front air knife and a back air knife. At both sides, a series of nozzles are installed to force excess zinc to flow back into the pot, by forming a high-velocity and horizontally extended gas jet (air or nitrogen) toward the moving strip. Each side was driven by two motors to regulate its gap to the centerline along which the strips pass. The air knife gap (distance between the nozzles and strips) and the air pressure (outlet air pressure from nozzles) are two major influencing factors of air-jet effect. Thus, the design of the coating weight control system is concerned mainly with the set of air knives under varying production conditions, with the objective to ensure that the thickness of zinc attached on the strip meets the requirements of customer orders.

However, the hot-dip coating process has some complicated characteristics such as a large time-

[‡] Corresponding author

 ORCID: Zai-sheng PAN, <http://orcid.org/0000-0003-1273-2519>
 © Zhejiang University and Springer-Verlag GmbH Germany, part of Springer Nature 2018

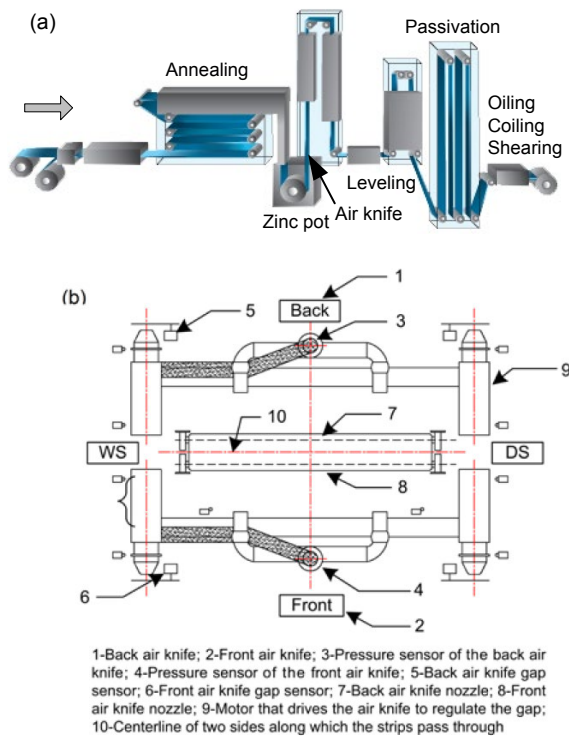


Fig. 1 Typical hot-dip galvanizing process (a) and the air knife (b)

varying lag, strong nonlinearity, and unmeasured disturbance, all of which lead to difficulty in controller design. So far, manual control has still been widely used in HDGLs. With the development of modeling techniques, many methods have been proposed to solve the nonlinearity and large measurement lag problems. These model-based control approaches can be divided into several categories, such as first principle (Thornton and Graff, 1976; Adams et al., 1996; Tu and Wood, 1996; Elsaadawy et al., 2007), regression (Shin et al., 2006; Guelton and Lerouge, 2010; Guelton et al., 2016), neural network (Bloch et al., 1997; Lu and Markward, 1997; Pal et al., 2006; Martínez-de-Pisón et al., 2010, 2011; Sanz-García et al., 2012), and model-free adaptive control with a Smith predictor (Zhang et al., 2011; Fei et al., 2016). Thornton and Graff (1976) first provided a coating weight model based on the maximum flux theory in which the jet effect is regarded as a body force. Tu and Wood (1996) improved the method by imposing shear stress on the surface of the liquid. Elsaadawy et al. (2007) developed a model that describes the pressure and wall shear stress distributions

as functions of the slot gap and impingement distance. On the basis of these models, the effect of each process variable on the coating weight can be calculated quantitatively and independently by the first principle. However, these models have difficulty in online control of the coating weight due to their complexity (Bloch et al., 1997; Shin et al., 2006).

Conversely, regression models (Shin et al., 2006; Guelton and Lerouge, 2010; Guelton et al., 2016) are simple exponential models whose parameters were tuned based on historical process data. Regression models can be easily realized, but the ability to generalize with respect to the nonlinear characteristics of the system is poor (Lu and Markward, 1997). Thus, as a powerful nonlinear learning technique (Yu and Li, 2008), a neural network is incorporated in the modeling of HDGL processes to deal with the complex nonlinear interrelations. Combined with other artificial intelligences such as the genetic algorithm (GA), the application results show huge advantages of neural networks in prediction accuracy, generalization ability, and computational complexity for online control compared with conventional regression approaches (Bloch et al., 1997; Pal et al., 2006; Martínez-de-Pisón et al., 2010, 2011; Sanz-García et al., 2012). However, as indicated by Guelton and Lerouge (2010), the coating weight on a galvanized strip is influenced by many factors, including some unmeasured variables like the crossbow and flatness of strips. Those unmeasurable external factors will reduce the prediction accuracy of the neural network and further affect the control performance (Lu, 1996; Lu and Markward, 1997). Also, the Smith predictor used by Zhang et al. (2011) and Fei et al. (2016) is sensitive to the modeling error and may not perform well in practice. All the above methods regard air pressure as the unique manipulated variable, while the air knife gap stays constant. However, based on practical experience, the air knife gap also plays an important role in the HDGL process, and a proper combination of the air knife gap and air pressure in a control strategy design will further help improve the control performance.

To enhance further the quality of the coating weight and reduce zinc waste, we present a novel neural network based coating weight control system composed of a feedforward control (FFC) and a feedback control (FBC). More specially, FFC

regulates both the air knife gap and air pressure when a drastic change occurs in the line speed or the target coating weight changes, while FBC regulates only the air pressure under relatively steady working status. The neural network with a bias-update is embedded in both FFC and FBC to manage the nonlinear process prediction and the large time-variant measurement delay problems.

The notations used in this paper are given in Table 1.

2 Problem statement

2.1 System analysis

A general model of a galvanizing plant, in terms of coating weight control, is summarized in the block diagram (Fig. 2). The coating weights are affected by several factors, and three main factors are the strip line speed, the air pressure, and the air knife gap. However, only the latter two are selected as manipulated variables (MVs) because the line speed depends on the capacity and the pace of upstream and downstream processes, which are measurable but uncontrollable. There are also other factors, such as air knife height, steel grade, and strip temperature, which are regarded as disturbances in the HDGL control system.

Although the current coating weight (CW) of a strip is determined by all the previously mentioned factors, immediately after the strip passes the air knife, it cannot be measured until the zinc cools from liquid to solid. Thus, the measurement equipment (X-ray coating gauge) is installed about 100 m away from the air knife, introducing a dynamic measurement delay τ (Fig. 2).

2.2 Control target

HDGL is a typical order-driven discrete-event production process, in which the target coating weight of each strip is determined by the customer demand and varies within a wide range. Thus, the first objective of the coating weight control system is to minimize the error between the target and the actual coating weight. In particular, negative error leads to off-specification products while positive error results in raw material (zinc ingots) waste.

On the other hand, order scheduling is determined by the customer order, due date, and product

inventory. It cannot be guaranteed that strips with the same target coating weight will be processed

Table 1 Notations used in this paper

Notation	Description
CV	Controlled variable
CW	Coating weight
CWd(t)	Predictive coating weight related to the current observed coating weight in bias-update
CWm(t)	Current observed coating weight at time t
CWp	Predictive coating weight
CWp'(t)	Corrected predictive coating weight at time t
D	Air knife gap
D_{error}	Input term of the derivative operator in the real-time optimizer
$D_{\text{FFC}}(t)$	Set point of the air knife gap in speed-FFC
D_{lower}	Lower bound of the air knife gap
$D_{\text{pre}}(t)$	Set point of the air knife gap in preview control at time t
D_{upper}	Upper bound of the air knife gap
I_{error}	Input term of the integral operator in the real-time optimizer
K_d	Derivative term
K_i	Integral term
K_p	Proportional term
MV	Manipulated variable
NNp	Neural network relationship
P	Air pressure
P_{error}	Input term of the proportional operator in the real-time optimizer
$P_{\text{FBC}}(t)$	Set point of air pressure in FBC
$P_{\text{FFC}}(t)$	Set point of air pressure in speed-FFC
P_{lower}	Lower bound of air pressure
$P_{\text{pre}}(t)$	Set point of air pressure in preview control at time t
P_{upper}	Upper bound of air pressure
Rfcw(t)	Future target coating weight at time t
Rcw(t)	Current target coating weight at time t
S	Line speed
t	Time
T_b	Piecewise constant function in calculating t_{vc}
t_{vc}	Optimal timing of the air pressure change in preview control
w_1, w_2	Two weights used in preview control
β	Weight coefficients in bias-update
τ	Measurement delay
ΔP	Predefined small disturbance term
ΔT	Sample cycle
Δu	Increment of air pressure in the real-time optimizer
Ω	Data set used to validate the NN model

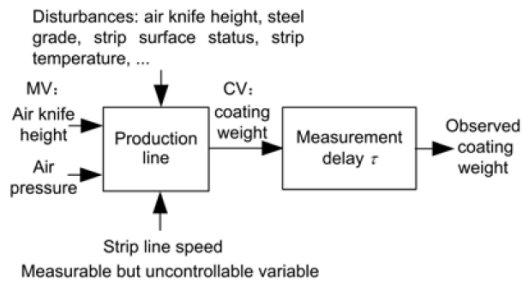


Fig. 2 Simplified block diagram of the coating weight control plant

successively, which leads to frequent changes in the target coating weight. Thus, it is important to minimize the transition time when the target coating weight changes. Shorter transition time means less raw material waste and fewer off-specification products.

2.3 Control difficulty

HDGL system has some complicated characteristics that lead to difficulty in coating weight control:

1. The X-ray coating gauge is installed far away from the air knife, inducing a large time-varying measurement lag.
2. Various external disturbances may have impact on model precision and control performance.
3. Strong nonlinearity makes it quite difficult to establish an accurate model covering all the operating points.
4. Due to the nature of the air knife, the settling time of air pressure is much longer than that of the air

knife gap which is driven by a motor, resulting in an unsynchronized regulation problem.

3 Design of the control system

3.1 Framework

A novel coating weight control system is proposed based on a neural network with the framework shown in Fig. 3. The control system has two work modes: FFC and FBC. FFC mode is activated when the line speed changes significantly or the set point of the coating weight is changed with a new strip. FFC can dramatically shorten the transition time when the set point of the coating weight changes, and can provide excellent disturbance rejection performance when the line speed changes. Considering the different characteristics of the air pressure and air knife gap, the execution logic of FFC mode is carefully designed.

A neural network, which is effective in describing the nonlinear characteristics of a real system, is incorporated in FBC to predict the value of the online coating weight. This predictive value instead of the measured coating weight is used as the feedback, so that the large time-variant measurement delay is avoided. In addition, the predictive coating weight (CWp) is modified through an online bias-update algorithm. Through this mechanism, the prediction error induced by the external disturbance can be reduced significantly. Based on this, a real-time

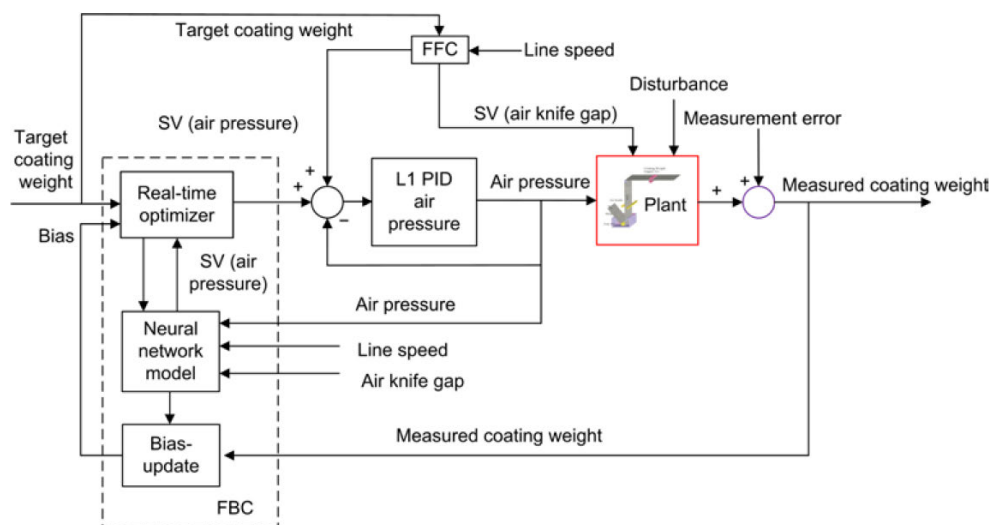


Fig. 3 Framework of the control system

online optimizer with excellent global search capability is employed to calculate the optimal set-point value of the air pressure.

To ensure proper control system operation, two control modes must not be run simultaneously and a well-designed logic must be used to determine the switching time between these two modes.

3.2 Neural network predictive model

The neural network predictive model was developed as the basis of FFC and FBC. It describes the nonlinear steady-state relationship between CWp and the manipulated variables (air pressure P and air knife gap D), with major measurable factors that will also have an effect on the coating weight, such as line speed S . Thus, the nonlinear mapping of the neural network can be described as follows:

$$\text{NNp}(P, S, D) = \text{CWp}. \quad (1)$$

Here, a three-layer neural network is adopted with three input neurons, one output neuron, and seven neurons in a hidden layer. The synaptic weights are optimized through off-line back propagation (BP) learning.

The target function that drives the training process is the error between CW and CWp in the training space, which includes four dimensions (air pressure, air knife gap, line speed, and actual coating weight).

From January 2016 to March 2016, about 780 000 actual process data pairs were obtained. The outlier and abnormal data were eliminated first. The representative samples covering all known production statuses were extracted from the remaining data through clustering. The NN toolbox in MATLAB 2008b was used to train the neural network automatically. Two-thirds of the samples were used as the training and validation set while the remaining one-third were used as the testing set. The root mean squared error (RMSE) was used to evaluate the models:

$$\text{RMSE} = \left(\frac{1}{|\Omega|} \sum_{s \in \Omega} (\text{CW}(s) - \text{CWp}(s))^2 \right)^{1/2}, \quad (2)$$

where Ω is the data set used to validate the models.

During the training, the learning rate in BP is set to 0.2, and the momentum is set to 0.9. Due to the

strong nonlinear mapping ability, the neural network can generate an accurate CWp value with a smaller prediction error, which is quite important for both FFC and FBC.

3.3 Feedforward control

3.3.1 Outline

In this study, FFC consists of two modules: preview control and speed-FFC. Preview control handles situations in which a new strip with a different target coating weight approaches the air knife, whereas speed-FFC works when the line speed changes significantly. Preview control calculates the optimal timing of air pressure change t_{vc} , the set point of air pressure $P_{pre}(t)$, and the air knife gap $D_{pre}(t)$, based on the predetermined production order sent from the L3 manufacturing execution system (MES). On the other hand, speed-FFC belongs to the typical feedforward approach, which is used to perceive drastic speed changes and adjust the MVs in advance to maintain the coating weight stability.

3.3.2 Preview control

When a strip with a different coating weight set point approaches the air knife, preview control (Fig. 4) is activated to regulate the air pressure and air knife gap. The objective of preview control is to switch the coating weight to the new set point as fast as possible.

As shown in Fig. 4, once preview control is activated, an optimization problem P1 is established and solved to derive the set points of $P_{pre}(t)$ and $D_{pre}(t)$. The detailed description of P1 is presented below:

P1: The major objective of preview control is to minimize the error between the future target coating weight $R_{fcw}(t)$ and CWp, which is calculated through the previously described neural network model depending on the current line speed $S(t)$ and the set points of $D_{pre}(t)$ and $P_{pre}(t)$, i.e.,

$$\min_{P_{pre}(t), D_{pre}(t)} |\text{NNp}(P_{pre}(t), S(t), D_{pre}(t)) - R_{fcw}(t)|. \quad (3)$$

The other objective is to minimize the gain of the coating weight and the air pressure at the current operation point, which will minimize the impact of natural fluctuations on the air pressure and further improve the production quality.

$$\min_{P_{\text{pre}}(t), D_{\text{pre}}(t)} \left| \frac{1}{\Delta P} \left[\text{NNp}(P_{\text{pre}}(t) + \Delta P, S(t), D_{\text{pre}}(t)) - \text{NNp}(P_{\text{pre}}(t), S(t), D_{\text{pre}}(t)) \right] \right|, \quad (4)$$

where ΔP is a predefined small disturbance term. By employing two weights, w_1 and w_2 , Eqs. (3)–(4) can be combined into a single one:

$$\min_{P_{\text{pre}}(t), D_{\text{pre}}(t)} \left(w_1 \cdot \left| \text{NNp}(P_{\text{pre}}(t), S(t), D_{\text{pre}}(t)) - \text{Rfcw}(t) \right| + w_2 \cdot \left| \frac{1}{\Delta P} \left[\text{NNp}(P_{\text{pre}}(t) + \Delta P, S(t), D_{\text{pre}}(t)) - \text{NNp}(P_{\text{pre}}(t), S(t), D_{\text{pre}}(t)) \right] \right| \right). \quad (5)$$

In addition, the following conditions should be met:

$$\begin{cases} D_{\text{pre}}(t) \in [D_{\text{lower}}, D_{\text{upper}}], \\ P_{\text{pre}}(t) \in [P_{\text{lower}}, P_{\text{upper}}], \end{cases} \quad (6)$$

where D_{lower} , D_{upper} , P_{lower} , and P_{upper} are the upper and lower bounds of the air knife gap and air pressure given in advance, respectively.

Essentially, conventional operational methods such as the Broyden-Fletcher-Goldfarb-Shanno (BFGS) algorithm and other quasi-Newton methods may be not applicable to P1 due to the implicit expression of the neural network mapping NNp and the strong nonlinearity involved in the objective. Thus, intelligence algorithms such as GA, simulated annealing (SA), and particle swarm optimization (PSO) can be used to solve the optimization problem P1 and derive the set points of MVs in preview control. Here, two different cases are considered in terms of the change direction of the target coating weight (Fig. 4):

Case 1: The target coating weight decreases. Fundamentally, when the target coating weight decreases, the air pressure should be increased. However, adjusting the air pressure is a slow process, while adjusting the air knife gap is instantaneous. Thus, the slow adjustment of the actual air pressure means that the actual coating weight can remain larger and converge to the target value slowly. In this case, the values of $D_{\text{pre}}(t)$ and $P_{\text{pre}}(t)$ derived from solving the problem P1 can be sent to L1 just when

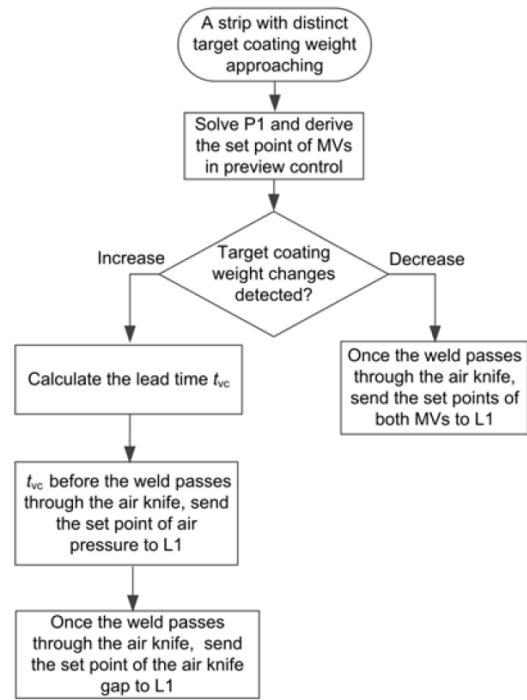


Fig. 4 Workflow of preview control

the weld passes through the air knife (i.e., when the target coating weight changes), thus creating $t_{\text{vc}}=0$.

Case 2: The target coating weight increases. When the target coating weight increases, the air pressure should be decreased. The slow air pressure adjustment process is ‘dangerous’ to the coating weight because the actual coating weight will stay below the target weight during this process, which is strictly forbidden in the transition. Thus, the air pressure should be regulated before the weld passes through the air knife, whereas the air knife gap is regulated when the target coating weight changes.

To calculate the lead time t_{vc} , problem P1 is solved to derive the air pressure $P_{\text{pre}}(t)$ and air knife gap $D_{\text{pre}}(t)$ based on the current line speed $S(t)$ and the future target coating weight $\text{Rfcw}(t)$. Then, we have

$$t_{\text{vc}} = T_b(|P_{\text{pre}}(t) - P(t)|), \quad (7)$$

where T_b is a piecewise constant function representing the settling time from the current air pressure $P(t)$ to $P_{\text{pre}}(t)$ approximately.

3.3.3 Speed-FFC

When a drastic change occurs in the line speed

$S(t)$, both the air pressure and the air knife gap should be regulated immediately to prevent large fluctuations in the coating weight. It is too late to regulate the MVs when the fluctuations are observed by the coating gauge several minutes later.

On the other hand, if a small change occurs to the line speed, the system will just regulate the air pressure alone by FBC.

The speed-FFC solves an optimization problem similar to that of preview control with the decision variables air pressure $P_{FFC}(t)$ and air knife gap $D_{FFC}(t)$, based on the current line speed $S(t)$ and the current target coating weight $R_{cw}(t)$. Here, the only difference between P1 and this problem is that the future target coating weight $R_{fcw}(t)$ is replaced by the current target coating weight $R_{cw}(t)$.

3.4 Feedback control with neural network

3.4.1 Outline

Different from the conventional FBC approaches which use the observed coating weight as the feedback information, a novel FBC framework is proposed using a bias-updated CW_p value rather than the actual value with a large time-variant delay (Yu and Li, 2008).

As stated previously, FBC is composed of a predictive neural network module, an online bias-update module, and a real-time optimization module. The detailed FBC workflow is shown in Fig. 5. The real-time optimizer generates the set point of the air pressure, and feeds it into the neural network model with the current knife gap and line speed. Then, the primitive CW_p from the neural network and the bias from bias-update module are added and fed back to the real-time optimizer. In this way, the set value of the air pressure is optimized iteratively until a satisfactory result is achieved.

3.4.2 Bias-update

The primitive $CW_p(t)$ is further corrected by an online bias-update module with the following workflow:

Step 1: Calculate the time delay corresponding to the current observed coating weight $CW(t)$. Fundamentally, this delay equals the travel time of the strip from the air knife to the coating gauge. Considering the simple relationship among the velocity, time, and distance in the first principle, the following equation

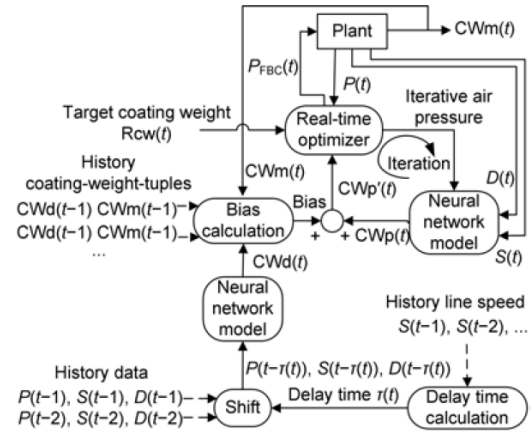


Fig. 5 Schematic of feedback control

can be obtained:

$$L = \sum_{k=0}^{\tau(t)} \Delta T \cdot S(t-k), \quad (8)$$

where ΔT is the sample time and $S(t)$, $S(t-1)$, ..., $S(t-\tau(t))$ are a series of line speeds at different sample time. The time delay $\tau(t)$ is computed as follows:

Initialization: define variable $L_{\text{sum}}=0$, $k=0$.

Step 1.1: Calculate $L_{\text{sum}}=L_{\text{sum}}+\Delta T \cdot S(t-k)$.

Step 1.2: If $L_{\text{sum}} < L$, let $k=k+1$, return to step 1.1; otherwise, go to step 1.3.

Step 1.3: Let $\tau(t)=k\Delta T$, and terminate the calculation.

Step 2: Shift the MVs and line speed by $\tau(t)$ in the time horizon and find the values of $P(t-\tau(t))$, $S(t-\tau(t))$, and $D(t-\tau(t))$ in the historical database. Fundamentally, the current observed coating weight $CW_m(t)$ is affected by these variables at time $t-\tau(t)$.

Step 3: Calculate the model predictive coating weight $CW_d(t)$ corresponding to the current observed coating weight $CW_m(t)$ using the past terms $P(t-\tau(t))$, $S(t-\tau(t))$, and $D(t-\tau(t))$:

$$CW_d(t) = \text{NNp}(P(t-\tau(t)), S(t-\tau(t)), D(t-\tau(t))). \quad (9)$$

Restore the coating-weight-tuple ($CW_m(t)$, $CW_d(t)$) in the database.

Step 4: Bias calculation. Based on a series of coating-weight-tuples in recent sample cycles such as ($CW_m(t)$, $CW_d(t)$), ($CW_m(t-1)$, $CW_d(t-1)$), ..., ($CW_m(t-N+1)$, $CW_d(t-N+1)$), a moving average method is used to calculate the adjusted model

predictive coating weight as follows:

$$\text{CWp}'(t) = \text{CWp}(t) + \sum_{k=0}^{N-1} \beta_k (\text{CWd}(t-k) - \text{CWm}(t-k)), \quad (10)$$

where β_k ($k=0, 1, \dots, N-1$) is a series of weight coefficients given in advance.

Different from the conventional approach of deriving the delay parameter approximately with the identification method as in the Smith predictor (Warwick and Rees, 1988), in bias-update algorithm the measurement delay of the coating gauge is derived precisely, so that the CWp is matched with the plant value by shifting the MVs and line speed. Based on these coating-weight-tuples, the corrected CWp (CWp'(t)) is derived. The prediction error caused by the inaccurate model, working condition changes, and other disturbances can be significantly reduced by bias-update.

3.4.3 Real-time optimizer

Based on the predictive model and bias-update, the optimizer calculates the set point of the air pressure, which minimizes the error between the target $\text{Rcw}(t)$ and the predicted coating weight CWp' with a given air pressure $P_{\text{FBC}}(t)$, that is,

$$\min_{P_{\text{FBC}}(t)} |\text{Rcw}(t) - \text{CWp}'|. \quad (11)$$

Given the current actual line speed $S(t)$, air knife gap $D(t)$, and the recent several coating-weight-tuples, the CWp' in Eq. (11) is a single-variable function of the variable $P_{\text{FBC}}(t)$ according to bias-update algorithm. However, due to the strong nonlinearity of the coating production line, it is difficult to find the optimal $P_{\text{FBC}}(t)$. To improve the FBC performance, a discrete proportional-integral-derivative (PID) controller based optimization approach is used to solve the above nonlinear problem. The workflow of the algorithm is as follows:

Initialization: Determine the proportional term K_p , integral term K_i , and derivative term K_d in PID. Let $P=P(t)$, the number of iterations $k=1$, the initial input terms $P_{\text{error}0}=0$, $I_{\text{error}0}=0$, $D_{\text{error}0}=0$, $P_{\text{error}1}=0$, $I_{\text{error}1}=0$, $D_{\text{error}1}=0$.

Step 1: Calculate bias-update predictive coating weight CWp'_k with P_k and the current actual plant

values such as $S(t)$ and $D(t)$, according to bias-update algorithm, and then $\text{error}_{k+1} = \text{Rcw}(t) - \text{CWp}'_k$.

Step 2: If error_{k+1} is less than a predefined threshold value, terminate the algorithm and return the current P_k as $P_{\text{FBC}}(t)$.

Step 3: $k=k+1$, and update the input terms of PID in incremental form as follows:

$$\begin{cases} P_{\text{error}_k} = \text{error}_k - \text{error}_{k-1}, \\ I_{\text{error}_k} = \text{error}_k, \\ D_{\text{error}_k} = \text{error}_k - 2\text{error}_{k-1} + \text{error}_{k-2}. \end{cases} \quad (12)$$

Step 4: The increment of air pressure is $\Delta u_k = K_p P_{\text{error}_k} + K_i I_{\text{error}_k} + K_d D_{\text{error}_k}$.

Step 5: $P_k = P_{k-1} - \Delta u_k$, and return to step 1.

3.5 Switch logic

The switch logic between FBC and FFC is carefully designed as shown in Fig. 6. The workflow of the switch logic can be summarized as follows:

Step 1: Judge the current status of the control system, if in FFC, go to step 2, and if in FBC, go to step 5.

Step 2: Judge whether a drastic change occurs to the line speed. If yes, regardless of whether the system is currently in preview control or speed-FFC, start the speed-FFC computation immediately and terminate the logic; otherwise, go to step 3.

Step 3: Judge whether the measurement coating weight (MCW) achieves a relatively stable value; i.e., the deviation of several consecutive MCWs is less than a given threshold value. If yes, go to step 4; otherwise, end the logic.

Step 4: Start FBC and terminate the logic.

Step 5: Judge whether any new strip with a different target coating weight approaches. If yes, start preview control and end the logic; otherwise, go to step 6.

Step 6: Judge whether a drastic change occurs in the line speed. If yes, start speed-FFC and end the logic; otherwise, end the logic immediately.

The switch logic workflow will be first executed during each control cycle. In addition, when the system is shifted from manual mode to automatic mode, the initial state of the control system is set to FBC to maintain system stability during the switch process.

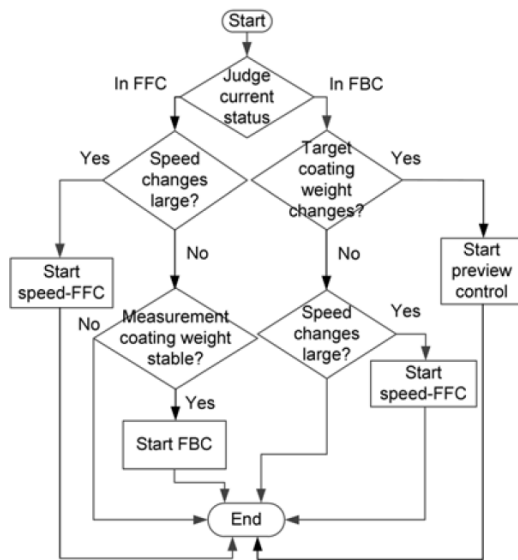


Fig. 6 Workflow of the switch logic

4 Application and results

4.1 System implementation

Based on the proposed algorithms, an HDGL control system was developed and implemented at VaLin LY Steel Co., Loudi, Hunan, China. The architecture of the control system is presented in Fig. 7.

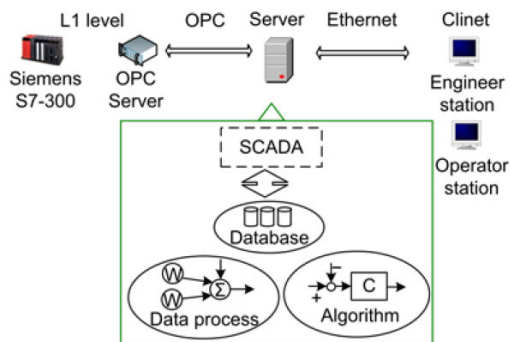


Fig. 7 Architecture of a real control system

The existing level I (L1 level) control system was implemented by a Siemens S7-300 PLC. Based on this control system, a supervisory control and data acquisition (SCADA) software was integrated to bridge the level I control system and the coating weight control system through OLE for process control (OPC), and to provide a human-machine interface (HMI). The coating weight control software was

coded in C++ and stored in an IBM X3650 server. In addition to FFC and FBC, several software modules were developed as follows:

1. Data gathering: collect and preprocess the actual process data.
2. Offline training: derive a good neural network model.
3. Strip tracking: track the processing strip on the HDGL to achieve the current target coating weight, strip thickness, and other information, and compute the distance between the weld and the air knife.
4. Manual/Auto switch logic: switch the mode of the control system between the manual and automatic modes without disturbance.
5. Performance analysis: collect the actual data related to the performance index online and do statistical analysis.
6. Heartbeat: test the connection status between the server and L1 level periodically, and switch the system to the manual mode immediately once the communications fail.

4.2 Parameter setting

After an online test for several weeks, the parameters included in the control system were optimized to achieve better control performance. The cycle of bias-update was set to 60 s. The control cycle was set to 5 s. The proportional term $K_p \in [0.1, 0.2]$, integral term $K_i \in [0.01, 0.02]$, and derivative term $K_d \in [0, 0.01]$ were set in the real-time optimizer.

4.3 Application results

4.3.1 Performance of bias-update

To show the effectiveness of bias-update, the online predictions of the coating weight before and after bias-update are compared in Fig. 8.

Within seven hours, the prediction before bias-update and the actual plant value were in substantial agreement, indicating that the neural network model is close to the practical system with a small modeling error. The prediction accuracy can be further improved using bias-update, in which the average error of the predicted value was significantly reduced from 2.26 g/m^2 to 0.54 g/m^2 .

4.3.2 Performance of preview control

To show the performance of preview control, the

process data of about 1 month measured by the coating gauge was collected. A transition began with the change of the target coating weight and ended when the actual coating weight fell within a target neighborhood ($[80, 85]$ for Z80, $[120, 125]$ for Z120), and the actual coating weight remained in the neighborhood for at least 200 s. The average transition time was significantly reduced by the proposed preview control from 580 s in the manual mode to 328 s in the automatic mode.

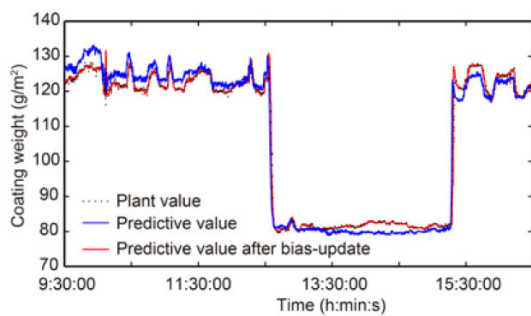


Fig. 8 Comparison of the predictive coating weight before and after bias-update (References to color refer to the online version of this figure)

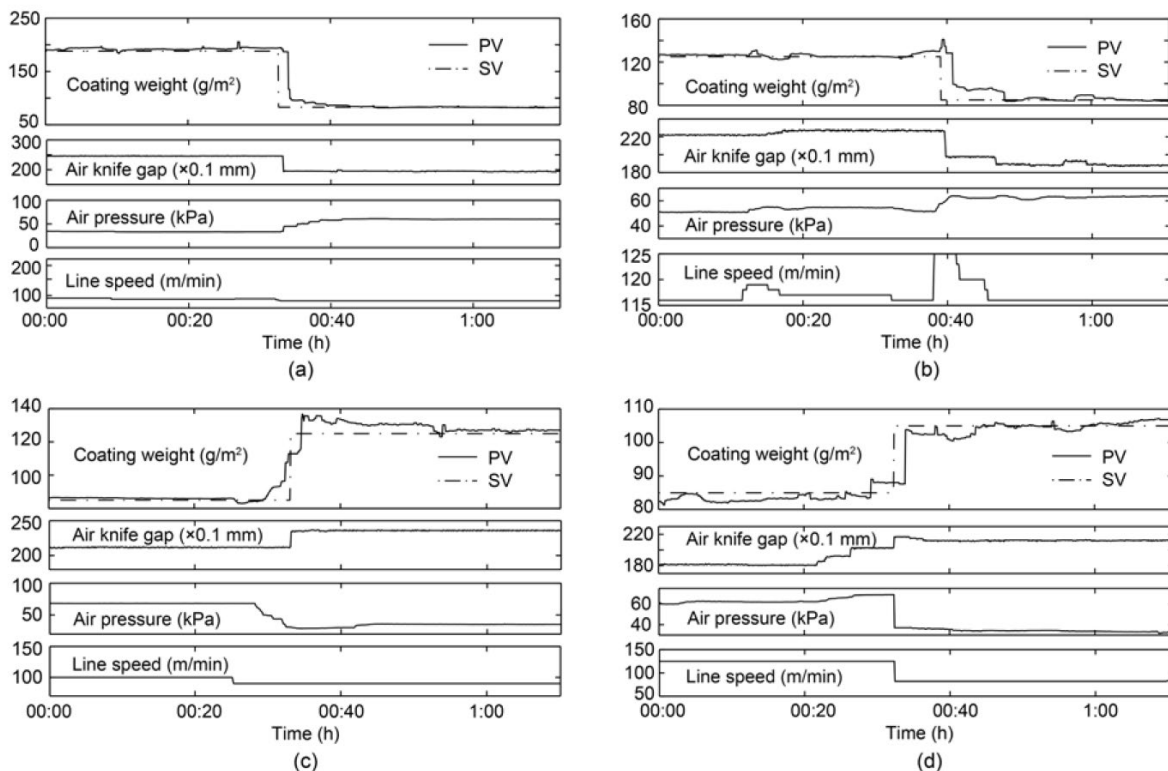


Fig. 9 Comparison between manual and automatic control during transition: (a) target coating weight decreases (automatic control); (b) target coating weight decreases (manual control); (c) target coating weight increases (automatic control); (d) target coating weight increases (manual control)

Four typical transition processes corresponding to the increase or decrease of the target coating weight under manual or automatic control were compared in Fig. 9. The transition time under automatic control was significantly shorter than that under manual control. In addition to the long transition time, the coating weight stayed below the target for a long time under manual control (Fig. 9d), and a large number of off-spec products were produced and wasted.

In Fig. 9a, the air pressure and air knife gap were regulated simultaneously once the target decreased, which forced the actual value to drop to the target quickly and then track smoothly the target without overshooting. On the other hand, as shown in Fig. 9c, the air pressure was regulated before the target changed, leading to a gradual increase in the actual coating weight. Meanwhile, the air knife gap was enlarged when the target changed. After that, the actual coating weight converged to the target quickly. Note that the coating gauge stopped working when a weld passed through it for the safety of the X-ray sensors. Thus, in both of the above cases, the measured value of the coating weight remained constant for a period of time.

4.3.3 Performance of feedback control

The data of seven successive days measured by the coating gauge with about half under manual control and half under automatic control was collected to evaluate the performance of FBC. The data corresponded to two main kinds of products, Z80 and Z120, with the target coating weights of 80 g/m² and 120 g/m², respectively. The probability density function (PDF) of the actual coating weight and its mean and variance were calculated based on different operational modes and product types (Fig. 10).

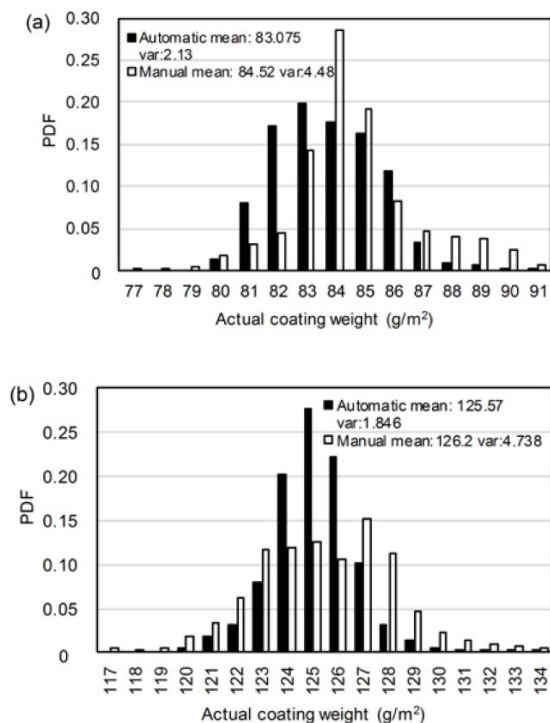


Fig. 10 Probability density function (PDF) of the actual coating weight with different operation modes and product types: (a) Z80 (automatic: 27 937 records; manual: 34 584 records); (b) Z120 (automatic: 19 125 records; manual: 29 094 records)

As shown in Fig. 10a, the coating weight under automatic control concentrated in a small area between 82 g/m² and 85 g/m² with an average of 83.075 g/m² and a variance of 2.13 g/m². In contrast, under manual control, more records were distributed above 84 g/m², especially above 87 g/m², which means more zinc was wasted, leading to an average of 84.52 g/m² and a variance of 4.48 g/m². It is obvious that auto-

matic control outperforms manual control in terms of Z80 strips.

Similarly, as shown in Fig. 10b, the coating weight under automatic control concentrated in a small area between 124 g/m² and 126 g/m² with an average of 125.57 g/m² and a variance of 1.847 g/m². In contrast, under manual control, the records were distributed with a larger average value of 126.2 g/m² and a larger variance of 4.738 g/m². Compared to the Z80 case, automatic control showed more significant improvement than manual control in the case of Z120.

Due to the decrease of production variance under automatic control, the set point of the target coating weight can be set closer to the product specification, and thus the passing rate can be further improved and the zinc material can be saved. Based on the mean and variance of the coating weight under both manual and automatic control, the potential zinc savings under the automatic control system can be calculated quantitatively.

The Z80 case is shown in Fig. 11a. The set point of Z80 can be decreased from 84.52 g/m² to 83.5 g/m², which creates zinc savings of 1.2% in Z80 production. Moreover, the area under 80 g/m² covered by the dashed line is smaller than that by the solid line, which means the passing rate will be improved. Similarly, as shown in Fig. 11b, the set point of Z120 can be decreased from 126.2 g/m² to 123.8 g/m², which creates zinc savings of 1.9% in Z120 production. According to the statistics in 2015, Z80 and Z120 made up about 90% of the total production and consumed 3120 and 3680 tons of zinc, respectively. Thus, a total of 107 tons of zinc can be saved per year, which is equivalent to about £200 000.

4.3.4 Long-term performance

The long-term performance of the proposed control system was evaluated based on the online running results during April 2016. The rate of automatic mode was about 80% where a total of 480 strips were produced, including 246 strips of Z80 and 206 strips of Z120. The statistical results were compared with the manual operation baseline before the implementation of the control system.

As shown in Table 2, in automatic control mode, the variance of the coating weight decreased by 52.8% and 14.6% for Z80 and Z120, respectively. This indicates that the fluctuation of the actual coating

weight in the production line decreased so that the quality of the products improved and more than 100 tons of zinc can be saved per year. Meanwhile, the average transition time was reduced by 43.4%. The experimental results on the real HDGL production line showed a great performance improvement compared with manual operation, which resulted in less quality fluctuation, shortened transition time, higher passing rate, and more zinc savings.

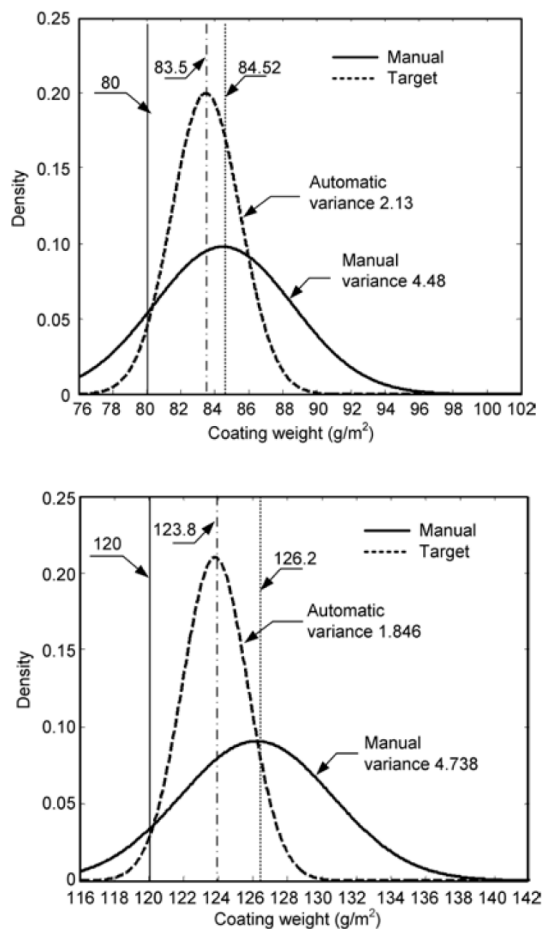


Fig. 11 Analysis on the zinc saving of Z80 (a) and Z120 (b)

Table 2 Performance comparison of the long-term run

Control mode	Variance of the coating weight (g/m²)		Average transition time (s)
	Z80	Z120	
Manual	6.44	4.19	580
Automatic	3.10	3.58	328

Z80 and Z120 represent two different kinds of strips with target coating weights of 80 g/m² and 120 g/m², respectively

5 Conclusions

In this study, we have proposed a novel neural network based coating weight control approach for HDGL. The system consisted of an FFC and an FBC, combined with a neural network predictive model, a bias-update module, and a real-time optimizer. Through this framework, four types of control difficulty—strong nonlinearity, large time-variant delays, strong disturbances, and unsynchronized regulation of two MVs—have been addressed.

The long-term industrial application results have shown the effectiveness and efficiency of the proposed method, and both the coating weight variance and the transition time were significantly reduced. About 107 tons of zinc can be saved per year, worth £200 000 according to statistical analysis.

Future work will include realizing automatic control of the production of Zn-Al coating strips and extending the control approach to other galvanized production lines such as those that produce galvanized pipe.

Acknowledgements

This research was partially based on the work done by Prof. Yongzai Lu with Zhejiang University, and the control system was further improved and implemented under his guidance. The authors would like to express their thanks to Prof. Lu for his great help.

References

- Adams J, Miles LB, Parker DJ, et al., 1996. Coating mass control on No. 2 galvanizing line at LTV steel's Indiana Harbor works. *Iron Steel Eng*, 73(1):123-131.
- Bloch G, Sirou F, Eustache V, et al., 1997. Neural intelligent control for a steel plant. *IEEE Trans Neur Netw*, 8(4): 910-918. <https://doi.org/10.1109/72.595889>
- Elsaadawy EA, Hanumanth GS, Balthazaar AKS, et al., 2007. Coating weight model for the continuous hot-dip galvanizing process. *Metall Mater Trans B*, 38(3):413-424. <https://doi.org/10.1007/s11663-007-9037-2>
- Fei J, Zhang Y, Wang JS, et al., 2016. Development and application of coating thickness control system for cold rolling continuous galvanizing line. *Iron Steel*, 51(5): 57-61 (in Chinese). <https://doi.org/10.13228/j.boyuan.issn0449-749x.20150388>
- Guelton N, Lerouge A, 2010. Coating weight control on ArcelorMittal's galvanizing line at Florange Works. *Contr Eng Pract*, 18(10):1220-1229. <https://doi.org/10.1016/j.conengprac.2010.05.008>
- Guelton N, Lopès C, Sordini H, 2016. Cross coating weight control by electromagnetic strip stabilization at the

- continuous galvanizing line of ArcelorMittal Florange. *Metall Mater Trans B*, 47(4):2666-2680.
<https://doi.org/10.1007/s11663-016-0672-3>
- Jordan CE, Goggins KM, Benscoter AO, et al., 1993. Metallographic preparation technique for hot-dip galvanized and galvanized coatings on steel. *Mater Charact*, 31(2):107-114.
[https://doi.org/10.1016/1044-5803\(93\)90051-V](https://doi.org/10.1016/1044-5803(93)90051-V)
- Lu YZ, 1996. Industrial Intelligent Control: Fundamentals and Applications. Wiley, New York, USA.
- Lu YZ, Markward SW, 1997. Development and application of an integrated neural system for an HDCL. *IEEE Trans Neur Netw*, 8(6):1328-1337.
<https://doi.org/10.1109/72.641456>
- Marder AR, 2000. The metallurgy of zinc-coated steel. *Prog Mater Sci*, 45(3):191-271.
[https://doi.org/10.1016/S0079-6425\(98\)00006-1](https://doi.org/10.1016/S0079-6425(98)00006-1)
- Martínez-de-Pisón FJ, Pernía A, Jiménez-Macías EB, et al., 2010. Overall model of the dynamic behaviour of the steel strip in an annealing heating furnace on a hot-dip galvanizing line. *Rev Metal*, 46(5):405-420.
<https://doi.org/10.3989/revmetalm.0948>
- Martínez-de-Pisón FJ, Celorrio L, Pérez-de-la-Parte M, et al., 2011. Optimising annealing process on hot dip galvanising line based on robust predictive models adjusted with genetic algorithms. *Iron Steel*, 38(3):218-228.
<https://doi.org/10.1179/1743281210Y.0000000001>
- Pal D, Datta A, Sahay SS, 2006. An efficient model for batch annealing using a neural network. *Mater Manuf Process*, 21(5):567-572.
<https://doi.org/10.1080/10426910600599356>
- Sanz-García A, Fernández-Cenicerós J, Fernández-Martínez R, et al., 2012. Methodology based on genetic optimisation to develop overall parsimony models for predicting temperature settings on annealing furnace. *Iron Steel*, 41(2):87-98.
<https://doi.org/10.1179/1743281212Y.00000000094>
- Shin KT, Park HD, Chung WK, 2006. Synthesis method for the modelling and robust control of coating weight at galvanizing process. *ISIJ Int*, 46(10):1442-1451.
<https://doi.org/10.2355/isijinternational.46.1442>
- Thornton JA, Graff HF, 1976. An analytical description of the jet finishing process for hot-dip metallic coatings on strip. *Metall Trans B*, 7(4):607-618.
<https://doi.org/10.1007/BF02698594>
- Tu CV, Wood DH, 1996. Wall pressure and shear stress measurements beneath an impinging jet. *Exp Therm Fluid Sci*, 13(4):364-373.
[https://doi.org/10.1016/S0894-1777\(96\)00093-3](https://doi.org/10.1016/S0894-1777(96)00093-3)
- Warwick K, Rees D, 1988. Industrial Digital Control Systems. IET, London, England.
- Yu W, Li XO, 2008. Optimization of crude oil blending with neural networks and bias-update scheme. *Eng Intell Syst*, 16(1):28-37.
- Zhang Y, Shao FQ, Wang JS, et al., 2011. Adaptive control of coating weight for continuous hot-dip galvanizing. *J Northeast Univ (Nat Sci)*, 32(11):1525-1528 (in Chinese).